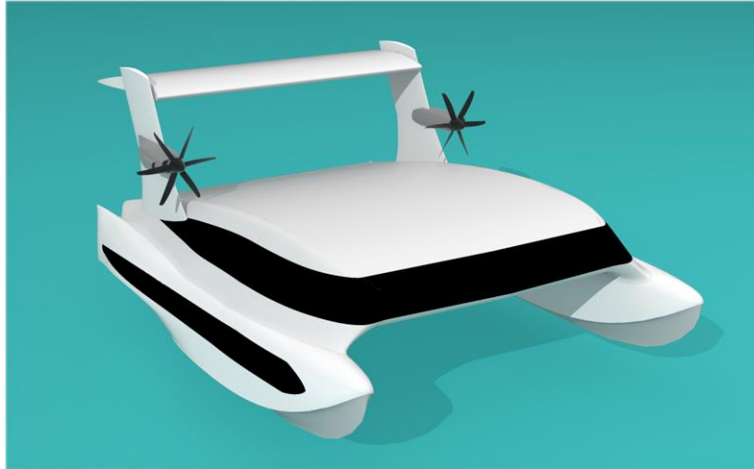


Aerodynamically Alleviated Marine Vehicle (AAMV): Bridging the Maritime-to-Air Domain

Daniel James, PE CEng MRINA and Maurizio Collu, PhD CEng MRINA
Cranfield University, UK



KEY WORDS

High speed marine vehicle; Wing-in-Ground effect; Aerodynamically Alleviated Marine Vehicle.

NOMENCLATURE

AAMV	Aerodynamically Alleviated Marine Vehicle
ACH	Aerodynamic Center in Height
ACP	Aerodynamic Center in Pitch
c	Chord (Mean Aerodynamic Chord)
C_L	Lift Coefficient
C_D	Drag Coefficient
C_M	Pitching Moment Coefficient
DHMTU	Department of Hydromechanics, Marine Technical University, St. Petersburg
GE	Ground Effect
h	Height Above Ground (from Trailing Edge)
NACA	National Advisory Committee for Aeronautics
OGE	Out of Ground Effect
RANS	Reynolds-Averaged Navier-Stokes
SST	Shear Stress Transport
WIG	Wing-in-Ground Effect

INTRODUCTION

As high performance marine vessels with improved performance characteristics are being requested by governments (DARPA 2015) and commercial operators, the Aerodynamically Alleviated Marine Vehicle (AAMV) provides a solution that combines speeds typical of rotary-wing and light fixed-wing aircraft with payload and loitering ability found in current high

speed craft. The innovative AAMV hybrid aero-marine platform utilizes an alternative implementation of wing-in-ground effect (WIG), a proven technology with a fascinating history of high speed marine operation.

This paper outlines some challenges and the work completed towards the development of a hybrid class of vessel that is able to bridge the maritime-to-air domain, comfortably operating in the water surface yet still delivering the speed of aircraft during an airborne cruise phase. An overview of current WIG design is briefly presented, leading to the conceptual approach for the AAMV. Development and assessment of the aerodynamic properties of the lifting surfaces are shown, with analysis of several wing profiles and their effect on the total lift force, drag force, and pitching moment that directly influence the stability characteristics of the vehicle. A methodology for sizing an appropriate platform is summarized, along with experimental results of a high speed hullform with characteristics suitable for this intended application. Finally, particulars of a potential AAMV are derived using an iterative numerical method and briefly compared to current craft.

The AAMV architecture can be applied across a range of traditional maritime applications, both military and commercial, advancing functionality and expanding the performance envelope of maritime craft. For close to a century, the influence of ground effect has promised economy for low-skimming flight over smooth water (Raymond 1921), a promise that has yet to reach its full potential.

BACKGROUND OF WIG

The first recorded vehicles specifically designed for the exploitation of ground effect were produced by Toivo Kaario in Finland, most notably an ‘Aerosledge’ built in 1935 for high speed travel over ice, with low aspect ratio main wing, single forward mounted propeller directly ahead of the wing, dual horizontal stabilizers extended far aft, with two narrow skis for ground contact (Rozhdestvensky 2006).

Numerous ground effect studies were conducted by the US Department of Defense during the decades of 1950-60s, although many configurations included discus-shaped geometries and annular jets. It was not until the 1960s that systematic WIG craft research and development began, led by chief designer Rostislav Alexeyev of the Central Hydrofoil Design Bureau in Nizhniy Novgorod, USSR. During an ambitious and well-funded program under the Soviet Navy, a series of prototypes and testing of various configurations led to the largest airborne vehicle of its era, the KM, popularly known in the west as the Caspian Sea Monster. The archetypal Alexeyev design features that characterize these vessels include a midship-mounted, low aspect ratio, rectangular straight main wing; large tail mounted horizontal stabilizer with substantial dihedral; well defined long and slender fuselage; and forward mounted engine thrusters, often having the thrust directed under the wing for power augmented ram (PAR) effect (Komissarov and Gordon 2010).

At a similar time, smaller scale WIG development was funded by the West German Ministry of Defence, who awarded contracts for several designs to Alexander Lippisch. The X-113 single-seat test craft was built in 1970 by Rhein Flugzeugbau GmbH (RFB), and following on from its success, the six-seat X-114 in 1977, as a prototype for coastal patrol duties. These craft shared a configuration comprising a fuselage with stepped planing lower surfaces, reverse delta main wing with significant anhedral and tapered chord, small tail surfaces, mounting a single propeller above the fuselage in a pusher configuration, and planing floats extending forward from the main wing tips. Noteworthy is the much smaller size of these craft; the maximum take-off weight of the largest was 1500 kg compared to 544 t for the Soviet KM (Yun et al 2010). A summary of the main conceptual differences between the Russian and German design families is shown below.

Table 2. Characteristics of typical Russian and German WIG craft

<i>Russian</i>	<i>German</i>
Low AR straight wing	Reverse delta wing
Zero sweep, taper, dihedral	Forward sweep, significant taper, anhedral
High wing loading	Low wing loading
Large tail OGE required	Smaller tail area can be used
Allows use of flapped wing, with separate elevator at tail	Small movement of CP through mode transitions, less control required
Typically longer, slender vessel	Typically more compact vessel
High speed design	Low speed design

Alternative Implementation

Although there are smaller WIG craft scattered throughout the world, built to various designs, very few have achieved the milestone of commercial viability. The most promising to date have been the descendants of the Lippisch vessels, most likely due to a combination of relatively stable and safe operation, prototype availability and smaller size that allows costs to remain manageable. However, the main technical problem in the development and commercialization of effective WIG is ensuring motion stability and good seaworthiness. Frequent crashes of WIG craft and high speed air-assisted boats demonstrate the importance of this problem (Matveev and Kornev 2011).

The fundamental causes of the majority of these accidents are control problems or structural failures due to insufficient strength for the loading experienced. Without resorting to exotic materials with extreme mechanical properties, the design of the vehicle should avoid inherently vulnerable geometry features. Existing WIG craft are generally not designed from a marine perspective and possess no real ability to withstand adverse waterborne conditions. As all of the previously described designs have experienced serious crashes, it may be that these aero-derivative forms are not best suited for the specific near-ground flight envelope.

Therefore, the current approach is to ensure the vessel geometry remains adequate to support marine environmental loading and can operate on the surface in wind and wave conditions that would exceed safe flying conditions. This philosophy leads to a vehicle that is primarily a high speed boat, but one that has its superstructure shaped in such a way that provides aerodynamic lift. This is the core ideology of the AAMV concept. To achieve this goal, three main objectives have been set out, as described below.

1. *Compact structure:* By incorporating design concepts developed for flying wing and blended-wing-body (BWB) aircraft, a more compact vessel can be produced minimizing structural vulnerabilities, i.e. long, slender fuselage or cantilevered tail arrangements. A tailless configuration would be ideal for reducing weight aft, aerodynamic drag, and the probability of structural failures.

2. *Utilization of internal volume:* Similar to the flying wing approach, a wing planform with long chord creates an internal volume that becomes useful for passenger and cargo transportation, even at moderate thickness to chord ratios. As the ground effect zone is given as a function of the normalized chord (or span) of the wing, larger overall dimensions result in a vessel that can operate with a greater height margin for a given sea state. These larger dimensions soon become an obvious location to house the vessel’s payload, eliminating the need for a conventional fuselage.

3. *Seakindly and efficient hull design:* Recent displacement hullform designs in the multihull sector have introduced slender hull concepts that are able to provide a suitable platform to attain

high speeds for passenger ferry and pleasure craft applications, whilst minimizing the extreme accelerations characteristic of planing craft. Additionally, these hulls are capable and efficient at lower speeds, instead of being constrained to a single design point. This type of flexibility is essential for AAMV operation, as a number of effective displacements, trim angles and powering requirements are experienced during the phases of operation.

The AAMV needs to perform successfully in a number of modes: low speed displacement and so-called semi-displacement waterborne modes; a transient condition defined by hydrodynamic and aerodynamic forces of the same order of magnitude (Collu 2009); and finally completely free of the water surface for high speed transit, fully airborne although not beyond the influence of the ground effect zone.

AERODYNAMIC PERFORMANCE

It is well-known that an aerodynamic lifting surface in close proximity to a ground plane offers an opportunity to achieve more efficient flight than is possible in free flight conditions (Wieselberger 1922). This efficiency comes in the form of increased lift for a given angle of attack and decreased induced drag. These characteristics were initially discovered empirically, then determined theoretically, and have been measured experimentally across a range of heights and wing aspect ratios (Fink and Lastinger 1961).

Longitudinal Static Stability

Stability in pitch has been identified as one of the key design parameters that are critical for success of WIG vehicles. The necessary proximity of the ground plane that offers the promise of increased aerodynamic efficiencies at flying heights not more than 10% of the wing chord, measured from the horizontal ground to the trailing edge of the foil, demands sufficient stability and control to avoid unintended physical contact with the ground surface (Korolyov 1998).

This proximity also complicates the equilibrium states necessary for stable operation, introducing the concept of an aerodynamic centre in height in addition to the more recognized and understood aerodynamic centre in pitch. The mathematical approach for the determination of pitch and height static stability for ground effect wings was begun by Kumar (1967) in his research at Cranfield College of Aeronautics, where the basic problem was framed and investigated. It was shown how the rearwards shift of the wing centre of pressure and the resulting change in pitching moment as the wing approaches the ground necessitates a centre of gravity position upstream of the aerodynamic centre to maintain pitching stability.

For any wing to be stable in flight, the response to any disturbance from an equilibrium steady state should be to return to the original position. This can be shown as:

$$\frac{dC_M}{d\alpha} < 0 \quad (1)$$

where dC_M is the change in pitching moment and $d\alpha$ is the change in angle of attack, or pitch angle.

The phenomenon of ground effect, by definition, states that there is an increase in lift as the distance to the ground plane decreases. This can be expressed as:

$$\frac{dC_L}{dh} < 0 \quad (2)$$

where dC_L is the change in lift coefficient and dh is the change in height above ground.

Irodov in the U.S.S.R. (1974) and Staufenbiel and Kleinedam in Germany (1980) independently further developed the mathematical framework to investigate static and dynamic longitudinal stability of WIG vehicles. It was shown that there is a change of pitching moment about the vessel centre of gravity with a change of height above ground, and what is termed a change in the position of the aerodynamic centre with height above ground. To ensure static stability, the relationships must follow:

$$\frac{\frac{dC_M}{d\alpha}}{\frac{dC_L}{d\alpha}} - \frac{\frac{dC_M}{dh}}{\frac{dC_L}{dh}} < 0 \quad (3)$$

Equation (3) can be simplified to show the position of the pitch and height centres must be located so that:

$$\bar{x}_p - \bar{x}_h > 0 \quad (4)$$

where \bar{x} indicates the position of the aerodynamic centres in pitch p , and height h , as measured from the leading edge and normalised against chord length.

Fig. 1 shows a graphical representation of the necessary positions of the aerodynamic centres in pitch and height, and body centre of gravity for airborne stability near the ground. The implications of these relationships permeate every aspect of the WIG craft and must be thoroughly understood before any meaningful progress can be made toward its development.

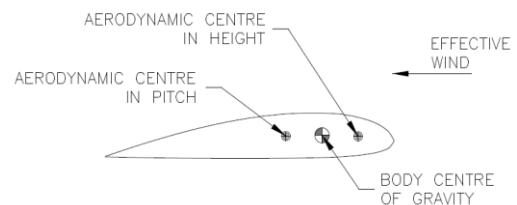


Figure 1. Critical positional relationship of aerodynamic and weight centres

Aerodynamic Surface Configuration

Many existing WIG craft have adopted fixed wing aircraft configurations, with identifiable fuselage, wing and empennage structures. Due to longitudinal stability requirements, many vessels use a large horizontal surface as tail, and this additional element decreases the overall aerodynamic efficiency of the vehicle. In order to minimize the size of the tail, S-shaped mean camber profile families have been designed (e.g. the DHMTU series) specifically for WIG configurations. Another solution has been to adopt a reverse delta configuration for the wing (i.e. Lippisch-type configuration). Despite the fact that a reflexed aerodynamic profile and a reverse-delta wing plan area have a lower efficiency than a clean profile with normal camber and plan area, they allow a substantial reduction of the tail horizontal area required, leading to an increased overall vehicle aerodynamic efficiency.

Alternative configurations have been investigated to address a loss of aerodynamic efficiency, trying to utilize geometries closer to a wing-body approach. For example, a multihull superstructure can be shaped as an aerodynamic profile, in order to exploit the large area available between the hulls and increase the ground effect due to the hulls acting as end plates. Such an approach was introduced with the 'Ekranocat' concept (Doctors 1997), where the effect of having aerodynamic lift sustaining a fraction of the vehicle weight was defined as 'aerodynamic alleviation'. Matveev and Dubrovsky (2007) presented a hybrid 1000 t trimaran that comprises three wave-piercing planing hulls and a wing-shaped superstructure: based on numerical simulations and aerodynamic experimental data, this configuration seemed to be characterized by a high overall efficiency and good seaworthiness, at speeds about twice those of contemporary fast ferries and combat ships.

Numerical Prediction

In order to realise a craft that makes effective use of the ground effect, it is necessary to acquire precise knowledge of how the lifting surface responds as the ground is approached; the exact change in lift and pitching moment has a significant effect upon the longitudinal stability of the vehicle, the change in drag affects powering, velocity and height (the amount of lift produced being a function of velocity).

In order to quantify these changes, a number of airfoil profiles have been modelled using computational fluid dynamics (CFD) software to determine the derived quantities of lift, drag and moment over a range of operational angles of attack (α) and heights above ground, normalised to chord length ($h/c = \bar{h}$).

A relatively simple profile with published performance data was selected for initial mesh setup and validation. A NACA 4412 cambered airfoil was chosen as this is one of the few profiles that has been compared experimentally and numerically, both in ground effect and in unbounded flow, with published results in the public domain. Additionally, this profile utilises an almost flat lower surface, beneficial in ground effect situations where a

Venturi effect can be set up by convergent-divergent flow under a more highly curved surface.

It was found that much less information has been published regarding computational analysis or experimental testing of airfoils in ground effect compared to unbounded flow conditions, even though the presence of the ground surface greatly influences the domain extents, mesh configuration and selection of boundary conditions.

A two-dimensional CFD domain was used to capture the aerodynamic sectional characteristics, utilizing the Reynolds-Averaged Navier-Stokes (RANS) equations, which approximate real-world three-dimensional unsteady flow with averaged, steady state solutions. The flow regime is considered low speed, where $Mach < 0.3$, so density variations due to pressure have been neglected resulting in an incompressible fluid approximation, i.e. constant density within any infinitesimal fluid element, with constant viscosity.

The underlying assumption of Reynolds averaging is that the time-variant turbulence can be approximated by decomposition into an averaged value and a fluctuating value. This introduces an additional term in the N-S equations, called the Reynolds stress, due to the shear-stress-like contribution of the fluid viscosity. As the RANS equations are not a closed set, it is not possible to solve for the Reynolds stresses directly; therefore, the formation of turbulent eddies in the near-wall region must be modelled mathematically. This requires the addition of a turbulence model.

A quantitative study of six turbulence models popularly used for external aerodynamic flows has shown that ground effect surface pressures were most accurately predicted with the SST $k-\omega$ model over all heights, and especially at lower heights with larger pressure gradients (Mahon and Zhang 2005). These turbulence models were all single and two-equation linear eddy-viscosity models, which included Spalart-Allmaras, standard $k-\epsilon$, standard $k-\omega$, SST $k-\omega$, $k-\epsilon$ RNG, and Realisable $k-\epsilon$. Therefore, the SST $k-\omega$ was the turbulence model used for the present analysis.

Mesh independence was assessed by building meshes consisting of three sizes of computational domain and four mesh refinement levels. Due to boundary layer considerations, the mesh in the immediate vicinity of the airfoil surfaces was varied only in the streamwise direction; the crossflow dimensions were determined by first layer height (y^+) requirements and inflation layer growth.

Several numerical studies of GE airfoils have used computational domains that could be considered insufficiently small when judged by conventional aerodynamic standards, for which boundaries are recommended to extend 10 to 20 chord lengths around the airfoil (ERCOFTAC 2000). Published WIG research has reported that a much smaller domain, e.g. extending $3c$ upstream of the leading edge, $5c$ downstream of the trailing edge, and $4c$ above the upper surface, has produced acceptable results (Abramowski 2007; Firooz and Gadami 2006).

A moving boundary with absolute velocity equal to the freestream flow was specified for the ground condition, as this has been shown to be most representative of experimental testing (Barber and Hall 2006).

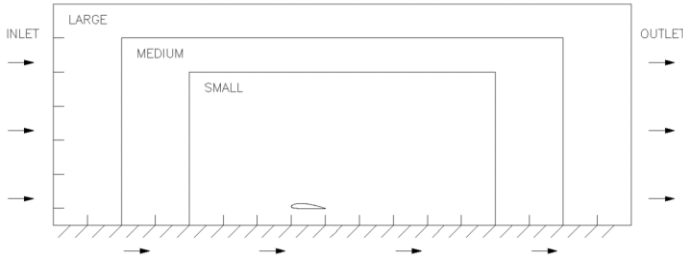


Figure 2. Graphical depiction of the three domain sizes

A rectangular domain was used for the three sizes, consisting of small, medium and large overall dimensions. The small size used the same distances as given in the WIG reports referenced in the preceding paragraphs, while the upwind and downwind dimensions were increased in increments of $2c$ and the upper boundary by $1c$ for the remaining two sizes. Four spatial resolutions were set up for each domain.

The range of C_L and C_M values varied less than 0.2% from the coarse mesh density to the extra-fine for the medium domain size, and slightly greater than 0.2% for the small and large domains. Drag values were within 2% for all resolutions of the small and medium domains, and under 3% for the largest domain.

The presence of the ground plane appears to stabilize the flow conditions around the airfoil to the extent that far-field effects become less significant. In practice, it is likely that even the smallest domain with the coarsest mesh resulted in force and moment estimations that would be of sufficient accuracy for many engineering applications. However, in the present work, the medium-size domain with a density around 200 000 nodes was selected as the default configuration, offering the most suitable trade-off of accuracy versus computational expense.

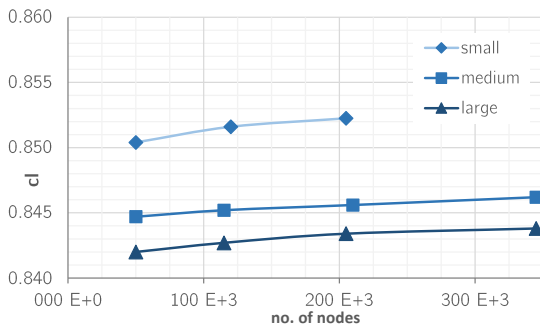


Figure 3. Lift coefficient dependency on mesh resolution

Ahmed, et al (2007) experimentally tested a NACA 4412 profile in a wind tunnel with moving ground, with particular emphasis on replicating two-dimensional flow. Lift and drag forces were measured, as well as pressure distribution over the upper and lower surfaces of the airfoil. As can be seen in Fig. 4, the trends

measured in these tests do not follow the expectation of increased lift as the distance to ground is decreased. It is not clear from the text why this occurred, but it has been shown that this reduction occurs in the case of a stationary ground plane (Hsiun and Chen 1996).

Additional NACA 4412 computational studies were then considered, such as Smith et al (2008) who conducted an analysis of two airfoil profiles in ground effect. An interesting feature of this analysis was the laminar flow regime enforced on the airfoil, even though the freestream $Re = 3 \times 10^5$ indicated transitional flow. This was done in an attempt to avoid the known overprediction of drag that is caused by implementing a turbulence model along the entire length of an airfoil. The results of this work were much closer to known values for unbounded flow and displayed the expected lift increase in the GE condition.

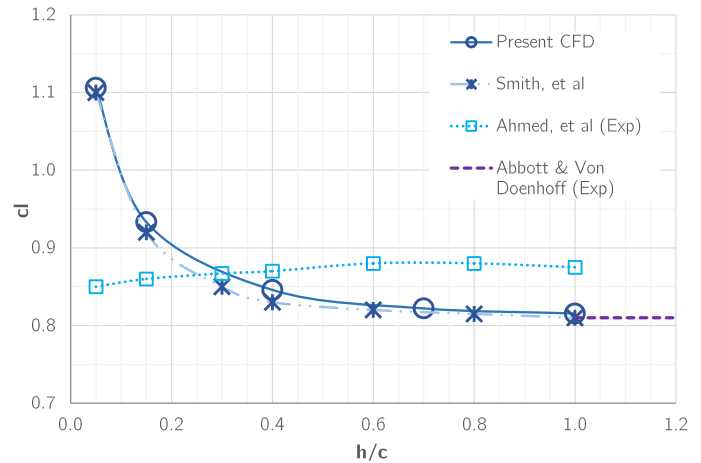


Figure 4. Lift coefficient comparison of NACA 4412, $\alpha = 4^\circ$

Although the NACA 4412 displays decent lift performance across a range of angles of attack and heights, it also produces a nose-down pitching moment. This moment requires additional control surfaces to ensure stable equilibrium for a given loading condition in GE. Typically, these control surfaces have taken the form of aft-positioned tails, as seen on conventional general aviation aircraft. These tails are placed outside of GE to ensure that the resultant control forces are not height-varying. This reduces the efficiency of the WIG craft as the tail produces additional drag, increases total weight, often requires a larger main wing due to the direction of the control forces, and does not take advantage of any lift increase or drag decrease due to GE.

Therefore, several other airfoil profiles were considered in order to assess their ability to generate a satisfactory lifting force but with a smaller moment, or ideally a nose-up pitching moment. The positive (nose-up) moment would allow for a tailless configuration that retains static stability, as shown graphically in Fig. 5.

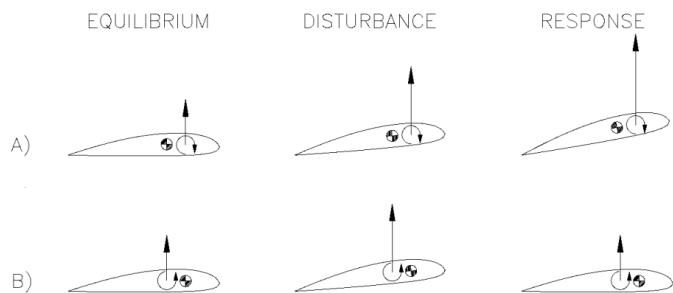


Figure 5. Disturbances from equilibrium result in instability in the upper series (A) and stability in the lower series (B)

The next profile to be considered was the NACA 25112, with 12% thickness and reflexed camber line. This profile also has a lower surface with more constant offset from the chord line, resulting in a flatter bottom without the droop at the forward end. The straighter section was expected to perform better at very low angles of attack, without causing downward suction due to the convergent-divergent flow restriction when placed close to the ground plane. The effect of the reflexed camber line is to reduce nose-down moment, but at the cost of reduced lift.

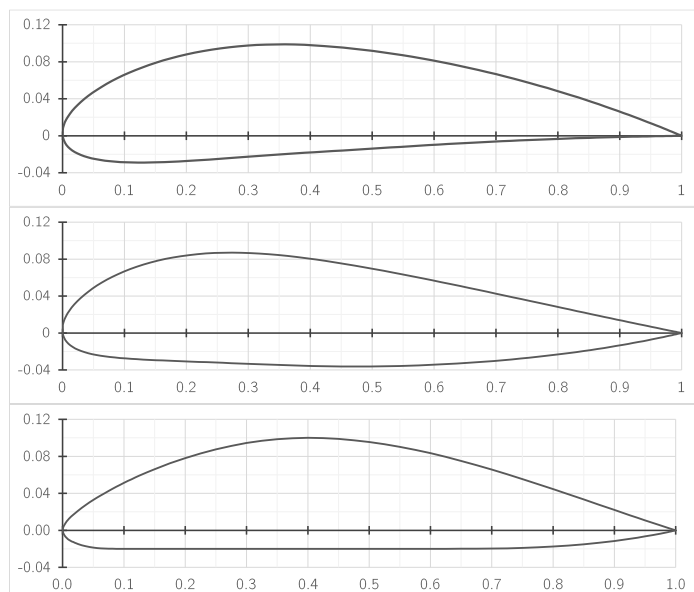


Figure 6. Airfoil profiles analyzed, from top: NACA 4412, NACA 25112, DHMTU 10-40.2-10.2-60.21.5

A family of airfoils specifically for WIG use was developed by the Department of Hydromechanics at the Marine Technical University, St. Petersburg (DHMTU) for the next-generation Ekranoplan program. These profiles are characterized by a reflexed camber line and flat, horizontal lower surface. The selection of the 10-40.2-10.2-60.21.5 profile was based upon the 12% thickness and long flat section along the bottom.

Each of the profiles were run over a range of normalized heights from 0.05 to 1.0, and angles of attack from -2° to 10° , representative of the likely operating range. Forces and moments

were measured about the trailing edges and converted to coefficient form based on freestream flow velocity and density.

The observed trends were quite consistent over the tested range, with the NACA 4412 producing greatest lift for a given angle over most of the height range. Fig. 7 shows typical lift curves for each of the profiles as a function of height.

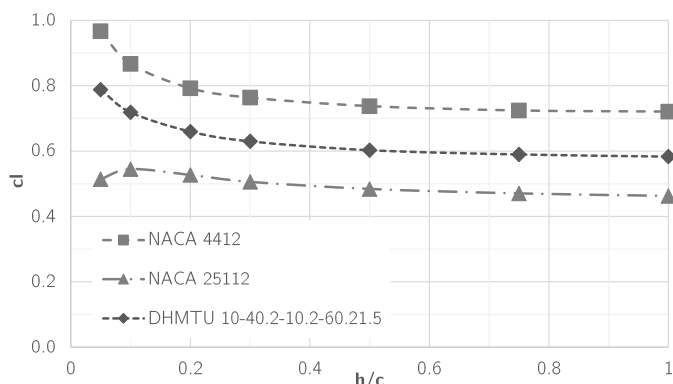


Figure 7. Lift coefficient comparisons of the three profiles, $\alpha=3^\circ$

The NACA 25112 at this angle displays a reduction in lift at the lowest height; this is also seen with the 4412 but not until $\alpha = 1^\circ$. Interestingly, the DHMTU profile also began to experience loss of lift around $\alpha = 1^\circ$, even though the flat bottom was intended to reduce negative effects at very low heights. Above these critical angles, all of the lift curves continued to rise as the ground was approached. Fig. 8 shows each profile at a different angle, one that results in comparable lift production, as seen in the upper plot. The DHMTU profile required an increase in angle of around 1° to produce similar lift to the 4412 profile, while the 25112 required an increase around 2° . This trend was fairly consistent across the range of angles.

The generated moments were compared for these respective angles, as shown in the lower plot. The 25112 produced the greatest positive (nose-up) moment across all heights. This characteristic would make it ideal for flying wing designs in unbounded flow conditions, but the loss of lift near the ground for moderate angles renders this profile unsuitable for GE use. The DHMTU profile also generated a greater positive moment than the 4412, the difference between the two increasing by slightly more than shown in the plot when adjusted for the contribution of the small lift increase of the 4412.

The DHMTU profile was selected for use in the AAMV numerical design model as its performance over the range of heights and angles was more consistent, not suffering from severe loss of lift in extreme GE, and the small but significant increase of nose-up moment resulted in a smaller tail surface being needed for static stability requirements.

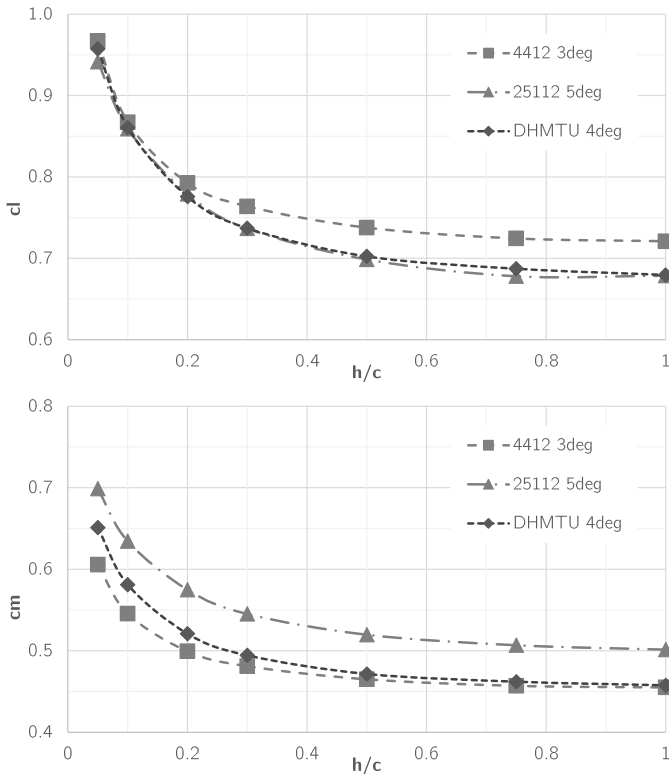


Figure 8. Lift (upper) and moment (lower) coefficients over the height range for the three profiles at comparative angles; note that moments are taken about the trailing edge

HYDRODYNAMIC PERFORMANCE

The high power required for take-off has proven to be one of the greatest impediments to the development of this type of vehicle (Rozhdestvensky 2006) as hydrodynamic resistance is typically the largest contributor to overall vessel drag during the transitional phases. This limits operation in increasing sea states and has often led to installed power in excess of cruise mode requirements.

There have been a number of configurations particular to WIG craft that have originated with the intent of reducing hump drag. Examples include vessels with stepped planing hulls incorporated into the underside of their fuselage, hydrofoil appendages, power augmented ram (PAR) employing forward mounted thruster engines that direct their exhaust under the main wing, and dynamic air cushion (DAC) that use similar techniques as conventional surface effect ships to encapsulate the oncoming air and maintain a high pressure zone on the underside of a lifting surface as the vessel moves forward.

However, the majority of existing WIG designs utilize planing surfaces to reach the speeds required to initiate aerodynamic lift. Whilst this may be the simplest arrangement to incorporate into a prospective design, it has contributed to the difficulty of take-off in waves, often exacerbated by unfavorable running trim. The transitional phases of take-off and landing are frequently categorized as the most difficult part of WIG design, with sea

state and environmental conditions given as primary factors (Yun et al 2010); therefore performance improvements in this area would be of foremost importance for a new design concept.

Alternative High Speed Hulls

Achieving the suitably high speeds required for take-off has typically been achieved through the use of hard-chine planing hullforms faired into the underside of the main fuselage. This geometry presents several significant disadvantages, such as extreme accelerations resulting from slamming and wave impact, strict longitudinal centre of mass (LCG) constraints with severe resistance penalties for forward locations, and inefficient operation at lower non-planing speeds.

A number of hullforms have been developed over the past several decades mainly for use in high-speed passenger ferry applications. These vessels are typically multi-hulled, with design specifications similar to that required for WIG use, such as being capable of attaining high speeds with reasonable fuel efficiency, and comfortable motions through a seaway with minimal slamming.

This style of displacement hull utilizes a very narrow beam to reduce wavemaking resistance, typically the highest component of drag at high speeds. The half-angle of entrance is very low, often resulting in wave-piercing characteristics. The slender vessel approach has successfully reduced wavemaking drag to the point that skin friction drag usually exceeds all other resistance components in the high speed range. Several examples of these craft are shown in Table 2, with their relevant particulars and performance characteristics.

As conventional marine vehicles, any lift that is produced to augment the hydrostatic buoyancy forces can only arise from the hydrodynamic flow, yet they are still capable of achieving length-based Froude numbers greater than one. If this type of performance were to be coupled to aerodynamic lifting surfaces, the apparent weight unloading would allow the craft to exceed these speeds as wetted surface is reduced, with very little additional power required due to the density differences between air and water.

Table 2. Performance characteristics of several slender-hulled high speed craft

Vessel	Speed	LWL	Power	F_{nL}	Disp.	Specific Power
	<i>kt</i>	<i>m</i>	<i>kW</i>	-	<i>t</i>	<i>kW/kg</i>
Francisco (Incat Ferry)	58	90.5	44000	1.00	1065	0.041
X-Craft	55	73	45000	1.06	900	0.050
Mary Slim VSV	38	22.5	1230	1.32	15	0.082

Additionally, the slender vessel approach permits more flexibility in LCG position, a critical parameter for WIG operation. Performance of planing hulls is known to be closely linked to LCG position, with very large resistance penalties for non-optimal forward positioning. Adverse handling has also proved to be a concern with forward LCG, resulting in a coupled longitudinal-transverse instability phenomenon (Savitsky 1985).

Therefore, it can be seen that an alternative hullform to the conventional hard-chine planing hull would be desirable, one that could accommodate a forward-positioned centre of gravity without adverse handling or resistance penalties, but also one that allows that vessel to achieve the required waterborne speeds. A more detailed description of the hullform design rationale and particulars of the geometry can be found in James and Collu (2015).

Experimental Testing

A model of 3 m LOA was constructed in the Ocean Laboratory workshop at Cranfield University, of glass reinforced plastic (GRP) over a CNC milled foam core; hand laid, vacuum bagged, and resin infused. The laminate schedule consisted of 2-4 plies (dependent on location) of 300 gsm E-glass in a 2/2 twill weave. Before lamination, a mounting plate was recessed into the deck amidships, bonded in and glassed over. The surface was finished to an approximate average roughness of 0.4 micron (240 grit sandpaper) and finished with a high gloss enamel coating.

For the initial tests it was decided to use a fully constrained towed rig, with the model positioned precisely to replicate specific displacement and trim combinations. The resulting forces and moments imposed on the model were measured to a calibrated accuracy of 0.75 N and 0.05 Nm respectively, using a six-axis force/torque transducer. Test runs were carried out in calm water at carriage speeds ranging from 1 m/s to 12 m/s.

The testing program matrix included four displacement conditions (with corresponding heights above datum) and three trim angles: 0°, 3°, 6° bow up. Multiple speed runs were carried out to assess the conditions most likely to be seen by each of the combinations. Ten unique configurations were tested in total. The model was designed to be suitable for scale factors between 5 and 10. Depending on the scale selected, the corresponding maximum full-size speeds tested would be between 52 kt and 74 kt.

Prediction of total free body resistance for the model configuration in the tested speed regimes was estimated prior to testing to be used as a form of comparative benchmark. The estimate was based upon slender body theory, characterized as a first principles potential flow approach to predict the far-field wave pattern. The contribution of viscous effects was estimated using a form factor multiplier on the frictional resistance of the static wetted surface area, as documented in the ITTC 1957 method. Although this form factor can be shown to vary with increasing speed, careful selection of a single average value for the entire range was expected to have a maximum error of +/- 5% (Molland et al 1994).

Initial results of the level trim resistance tests is shown in Fig. 9, along with the nominal prediction line for the full displacement condition. The model appears to perform slightly better than expected at lower speeds before a rapid drag increase around 9 m/s, however as the bodily sinkage was fully constrained it is likely a free body test would demonstrate a heavier effective displacement and higher drag values.

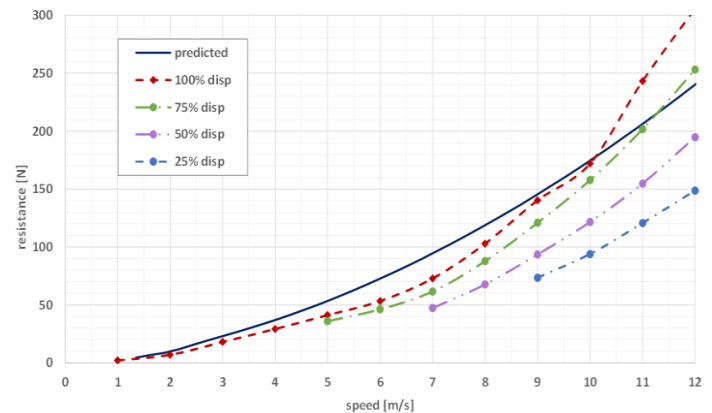


Figure 9. Results of the even keel performance at four displacements

Spray rails, or any other method for the reduction of side wetting, were not installed on the model. Images and video from the tests show considerable rise of the bow wave up the topsides at many of the higher speeds. The control of side wetting in future tests would be expected to reduce skin friction drag and provide additional lift.

The curves represent the four tested displacement conditions, in order to represent stages of aerodynamic alleviation ratios, defined as the total aerodynamic lift divided by the vehicle weight, as experienced during a take-off evolution. The lower part of the speed range is where the vessel would be entirely hydrostatically and then hydrodynamically supported. As forward speed increases, aerodynamic alleviation of the vessel weight would occur, effectively reducing the displacement.

The upper part of the speed range would correspond to conditions where aerodynamic lift is significant, with the result that the predicted drag would effectively skip to the next curve to the right hand side, representative of the newly unloaded condition. For a given power, the ongoing lowering of hydrodynamic resistance should allow the craft to accelerate rapidly, further generating aerodynamic lift until water contact diminishes entirely at lift-off.

DESIGN METHODOLOGY

According to standard naval architectural design practice, a holistic approach represented by the design spiral of Fig. 10 has been carried out in order to fully integrate all mission requirements and design constraints into a final AAMV configuration. The main idea was to define the vehicle operational requirements, leading to the identification of any necessary design constraints. In a previous paper, the complete procedure has been illustrated, detailing the approaches for each step of the spiral design (Bertani et al 2014). For the present work, a simplified approach has been adopted, since the focus of the analysis is on the performance of the hull tested in the experiments, described above.

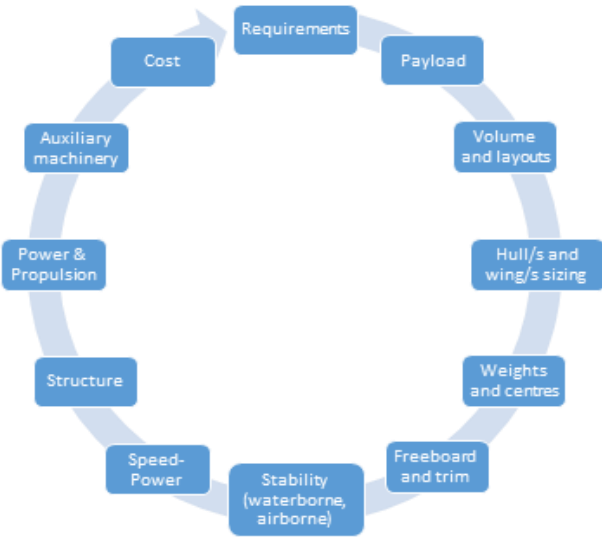


Figure 10. AAMV design spiral [courtesy of Renaissance Design (UK) Ltd]

The requirements are a simplified set, consisting of range (800 nm), take-off speed (50 kt), and airborne cruise speed (120 kt). The payload is specified only as a total weight (3000 kg). Furthermore, rather than performing a detailed scantling calculation for the hulls and wing (‘Structure’ step in Fig. 10), the structural weight is assumed to be a percentage of the total weight, 45%, based on typical percentages for WIG vehicles (Yun et al 2010). Similarly, the weight of the auxiliary machinery and ancillaries are estimated as 15% of the total weight.

Another very important aspect, determining the equilibrium attitude in waterborne conditions and stability in airborne conditions, is the position of the centre of gravity (CG). For the present analysis, the longitudinal (from stern, positive forward) and vertical (from keel, positive up) has been specified. All the other steps are implemented as illustrated in the previous work (Bertani et al 2014).

Waterborne equilibrium attitude estimation

The longitudinal (surge, heave and pitch) equations of equilibrium for an AAMV configuration have been defined in Collu et al (2009), taking into account the simultaneous

contribution of hydrostatic, hydrodynamic, and aerodynamic forces. Originally, in order to estimate the hydrostatic and hydrodynamic contributions, the Savitsky method was adopted, since the hull considered was a simple prismatic planing hull. Due to the limitations of the Savitsky approach, it would be difficult to estimate the hydrodynamic forces for the present hull.

The alternative would be to evaluate the hydrostatic and hydrodynamic contribution experimentally or numerically; for the present approach, the experimental data obtained in the aforementioned testing have been complemented with numerical results obtained with the code Autowing (Icarus Marine). Autowing is based on the method of discrete vortices (vortex lattice method) and is capable of modelling complex aerohydrodynamics of high-speed craft and wing in ground effect vehicles.

For the considered hull, a database of hydrodynamic lift, drag, and moment coefficients is calculated, having as input the displacement (draft) at zero speed and the trim angle, for a range of Froude numbers. This approach is slightly different from the one presented in James and Collu (2015), where experimental data from NACA seaplane hulls were used.

CASE STUDY

The design spiral approach has been implemented in MATLAB®; at the end of each iteration, the updated mass and installed power are compared against the values obtained in the previous iteration, and if the difference is below a threshold (5% for the present analyses) the iteration is stopped, otherwise further iterations are performed until convergence. The characteristics of the studied configuration are presented in the table below.

Table 3. Particulars of representative AAMV

REQUIREMENTS				
MAIN				
Payload	3000	kg		
Range	800	nm		Range
Take off speed	50	kt		Take-off speed
Airborne cruise speed	120	kt		Cruise speed in WIG mode
VEHICLE CHARACTERISTICS				
VEHICLE: INERTIAL				
Mass	12.332	t		Total mass
LCG	7.18	m		Longitudinal position of CG (from transom)
VCG	0.45	m		Vertical position of CG (from keel)

VEHICLE: GEOMETRY				
LOA	17.95	m	Total length of the vehicle	
Width	9.62	m	Total width of the vehicle	
Draft	0.45	m	Draft	
HULL/S				
Number	2	\	Number of hulls	
Length	17.95	m	Hull LOA	
Beam (single)	1.5	m	Hull beam (single)	
Beam (tot)	9.62	m	Hull beam (total)	
WING/S				
Wing length (mac)	17.95	m		
Wing span	6.63	m		
Wing profile		\	DHMTU	
LAC	13.46	m	Longitudinal position of AC from transom	
VAC	7.18	m	Vertical position of AC from keel	
ETA	2	deg	Angle between keel and mac	
POWER AND PROPULSION				
Propulsion type	Aero Turbo-prop	\	Type of propulsion	
Total power	2126	kW	Total power installed	
Number of engines	2	\	Number of engines	
PERFORMANCE RATIOS				
F _{nl}	4.65	\	Length-based Froude number (cruise)	
F _{nv}	12.97	\	Volume-based Froude number (cruise)	
Specific Power	0.172	kW/kg	Power per unit mass	
Transport Factor	3.51	\	Speed x Weight / Power	

Although direct comparison with existing vessels can only be approximate at this stage, a vehicle with these particulars would offer not only significantly increased speeds, but also increased transport efficiency, a measure that combines speed, total weight and installed power. A modified version of Almeter's (2008) plot of transport efficiencies, or transport factor (TF), for current vessels is presented in Fig. 11, with the AAMV marked with a star. It can be seen that the AAMV delivers a TF greater than that achieved by any other surface-effect craft, beyond their technological limitations.

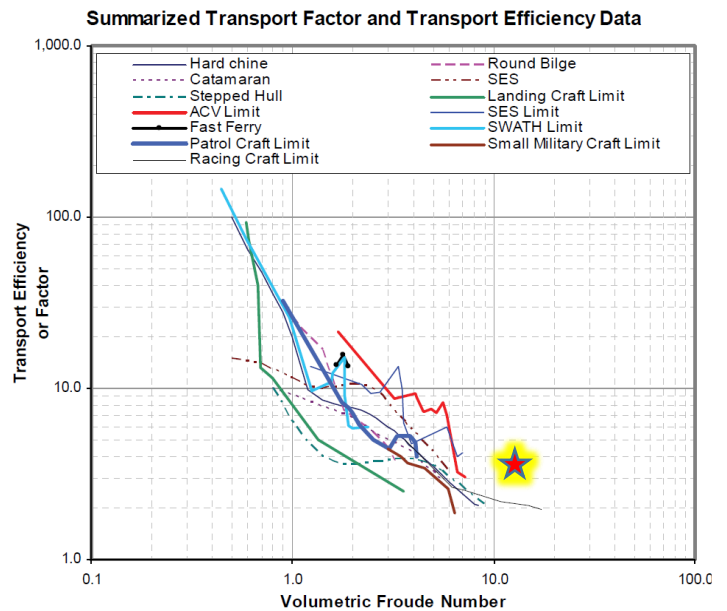


Figure 11. AAMV transport efficiency comparison to existing marine craft (modified from Almeter 2008)

Furthermore, the IMO regulatory framework for Type B WIG allows these craft to be constructed, operated and maintained in accordance with maritime regulations, avoiding a much costlier involvement with civil aviation authorities.

CONCLUSIONS

This paper has described the concept of the AAMV and some of the work currently being carried out to understand the physical principles involved and to formulate a design methodology to produce such a vehicle. There are many applications for the AAMV, with various militaries interested in WIG capability for mission scenarios such as heavy lift applications, rapid response search-and-rescue, and delivery of special forces equipment and personnel.

On the commercial side, current options for personnel transfer to offshore oil and gas fields and wind farms are generally limited to either relatively slow and often uncomfortable crew boats, or expensive and often dangerous helicopter transit. Passenger ferry service providers and the luxury yacht sector are consistently looking for faster, cheaper or more efficient vessels, or even new and novel craft that provide an advantage over their competitors.

The AAMV can be considered a third transportation option, one that combines the speed and comfort of an aircraft above the water surface, with the waterborne performance and operational costs associated with high performance marine vehicles. In many current and past WIG craft, aerodynamic aspects have governed the design, leading to poor resistance and manoeuvrability characteristics during waterborne operation.

A true AAMV should be fully operational as a marine vehicle, something that existing aero-derivative designs have not been able to achieve. By applying the concepts presented in this paper, we demonstrate the technical feasibility and operational potential in realizing this type of vessel.

REFERENCES

Abramowski, T. 'Numerical investigation of airfoil in ground proximity.' *Journal of Theoretical and Applied Mechanics*, 45(2), pp. 425-436, 2007.

Ahmed, M.R., Takasaki, T. and Kohama, Y. 'Aerodynamics of a NACA 4412 airfoil in ground effect.' *AIAA Journal*, 45(1), 2007.

Almeter, J. 'Avoiding Common Errors in High-Speed Craft Powering Predictions.' *6th Int. Conference on High-Performance Marine Vehicles*, Naples, 2008.

Barber, T., and Hall, S. 'Aerodynamic Ground Effect: A case-study of the integration of CFD and experiments.' *Int. Journal of Vehicle Design*, January 2006.

Bertani, M., Collu, M., Pensa, C., Rizzo, C.M. 'Preliminary scantling design of Aerodynamically Alleviated Marine Vehicles (AAMV).' *10th Symposium on High Speed Marine Vehicles*, Naples, Italy, 2014.

Collu, M., Patel, M.H. & Trarieux, F. 'The longitudinal static stability of an aerodynamically alleviated marine vehicle, a mathematical model.' *Proceedings of the Royal Society A: Mathematical, Physical and Engineering Sciences*, 466(2116), pp.1055–1075, 2009.

Collu, M., Williams, A.G.W., Patel, M.H., Trarieux, F. 'Aerodynamically Alleviated Marine Vehicles (AAMV): Development of a Mathematical Framework to Design High Speed Marine Vehicles with Aerodynamic Surfaces.' *High Performance Marine Vessels Conference (HPMV'09)*, RINA, Shanghai, China, 2009.

DARPA. *Broad Agency Announcement: Innovative Systems for Military Missions*. BAA-14-25, 2015.

Doctors, L. 'Analysis of the efficiency of an ekranocat: a very high speed catamaran with aerodynamic alleviation.' *Int. Conf. on Wing in Ground Effect Craft*, London, UK, 1997.

ERCOFTAC Special Interest Group on 'Quality and Trust in Industrial CFD.' *Best Practice Guidelines*, ver. 1.0, January 2000.

Fink, M. P. and Lastinger, J. L. 'Aerodynamic Characteristics of Low-Aspect-Ratio Wings in Close Proximity to the Ground.' *NASA Technical Note D-926*, July 1961.

Firooz, A. and Gadami, M. 'Turbulence Flow for NACA 4412 in Unbounded Flow and Ground Effect with Different Turbulence Models and Two Ground Conditions: Fixed and Moving Ground Conditions.' *Int. Conf. on Boundary and Interior Layers*, BAIL, 2006.

Hsiun, C. M. and Chen, C. K. 'Aerodynamic Characteristics of a Two-Dimensional Airfoil with Ground Effect.' *Journal of Aircraft*, vol. 33, no. 2, March-April 1996.

http://icarusmarine.com/index_files/autowing.htm

Irodov, R.D. *Criteria of the Longitudinal Stability of the Ekranoplan*, Ohio, 1974.

James, D. and Collu, M. 'A Novel Design for an Offshore Wind Farm Vessel: Application of the AAMV.' *Design & Operation of Wind Farm Support Vessels*, RINA, London 2015.

Komissarov, S. and Gordon, Y. *Soviet and Russian Ekranoplans*. Midland Publishing, Surrey, 2010.

Korolyov, V.I. 'Longitudinal Stability of Ekranoplans and Hydrofoil Ships.' *RTO-AVT Symposium on Fluid Dynamics Problems of Vehicles Operating Near or In the Air-Sea Interface*, Amsterdam, 5-8 October 1998.

Kumar, P.E. 'Stability of Ground Effect Wings.' *Cranfield College of Aeronautics, Report Aero No. 196*, 1967.

Mahon, S. and Zhang, X. 'Computational Analysis of Pressure and Wake Characteristics of an Aerofoil in Ground Effect.' *Journal of Fluids Engineering*, vol. 127, March 2005.

Matveev, K.I. & Dubrovsky, V. 'Aerodynamic characteristics of a hybrid trimaran model.' *Ocean Engineering*, 34(3-4), pp.616–620, 2007.

Matveev, K.I, and Kornev, N. 'Dynamics and Stability of Boats with Aerodynamic Support.' *11th International Conference on Fast Sea Transportation*, Honolulu, USA, September 2011.

Molland, A.F., Wellicome, J.F. & Couser, P.R. 'Resistance Experiments on a Systematic Series of High Speed Displacement Catamaran Forms: Variation of Length-Displacement Ratio and Breadth-Draught Ratio.' *Ship Science Report No. 71*, University of Southampton, 1994.

Raymond, A.E. 'Ground Influence on Aerofoils.' *NACA Technical Note No. 67*, December 1921.

Rozhdestvensky, K. V. 'Wing-in-ground effect vehicles.' *Progress in Aerospace Sciences*, 42(3), pp.211–283, 2006.

Savitsky, D. 'Planing Craft.' *Modern Ships and Craft*. Naval Engineers Journal, Vol. 97, Issue 2, American Society of Naval Engineers, 1985.

Staufenbiel, R. 'Longitudinal motion of low-flying vehicles in nonlinear flowfields.' *Proceedings of the Congress of the International Council of the Aeronautical Sciences*. Munich, pp. 293–308, 1980.

Wieselsberger, C. 'Wing Resistance Near the Ground.' *NACA TM-77*, 1922

Yun, L., Bliault, A. & Doo, J. *WIG Craft and Ekranoplan*. Springer, 2010.